

# Preparation of $\text{Ag}_{5-x}\text{Te}_3$ Thin Films and Confirmation of Their Crystal Structure by High Resolution Electron Microscopy

Walter Kälin and John R. Günter<sup>1</sup>

*Institute for Inorganic Chemistry, University of Zürich, Winterthurerstr.190, CH-8057 Zürich, Switzerland*

Received November 29, 1995; accepted February 28, 1996

DEDICATED TO PROFESSOR H. R. OSWALD ON THE OCCASION OF HIS 65TH BIRTHDAY

Single crystalline thin films of  $\text{Ag}_{5-x}\text{Te}_3$  (Stuetzite) have been prepared from thin silver films and tellurium vapour and their crystal structure is compared to crystal structures formerly determined by various authors using X-ray and electron diffraction. The occurrence of one of these structures in our films is confirmed by means of electron diffraction and high resolution electron microscopy with image simulation, whereas others could be rejected. These thin films crystallize in the  $P\bar{6}2_m$  space group with  $a = b = 1.3456(9)$  nm and  $c = 1.6917(9)$  nm. The crystal structure of  $\text{Ag}_{5-x}\text{Te}_3$  ( $x = 0.47$ ) can be described as a superstructure of tellurium. The lattice constants  $a$  and  $b$  of the basic tellurium structure are modulated with a period of 3. Each third spiral chain of the tellurium crystal structure is retained in the tellurium sublattice of  $\text{Ag}_{4.53}\text{Te}_3$ . Along  $[00z]_{\text{Ag}_{4.53}\text{Te}_3}$ , the tellurium chains are elongated by 36% in comparison to  $[00z]_{\text{Te}}$ . © 1996 Academic Press, Inc.

## INTRODUCTION

Silver chalcogenides are known to be fast ionic conductors or semiconductors and as such find practical applications in silver photography as sensitizers or in optics and microelectronics as rewritable storage media.

In order to understand these properties, an exact knowledge of their crystal structure is indispensable. However, it has been found that, e.g., silver sulfide (1) or silver selenide (2) in the form of very fine particles or thin films exist in metastable forms different from the stable structures found in the bulk. No such findings have been reported for silver tellurides yet, but for the phase known as stuetzite, of the composition  $\text{Ag}_{5-x}\text{Te}_3$ , even the structure of the stable form is controversial. In a broader study on silver telluride thin films (3), we have therefore attempted to clarify the nature of thin films of stuetzite.

In the literature, the room temperature structure of  $\text{Ag}_{5-x}\text{Te}_3$  has been described by several authors as hexago-

nal, with  $a = b \cong 1.34$  nm and  $c \cong 0.85$  nm (Table 1). Only Peters (4) has reported a doubled  $c$ -axis with 1.69 nm. The stuetzite phase represents a phase of structural cation disorder at room temperature having a silver deficit in relation to the stoichiometric composition  $\text{Ag}_5\text{Te}_3$  (5). Its silver content depends on the reaction conditions and the preparation methods. The phase transition to a high temperature phase and the thermodynamic properties have recently been studied by Gobec and Sitte (6).

For the stuetzite phase, there are two distinctly different reports on the atomic configuration within the hexagonal unit cell (7, 8) and a more recent one which is, however, not easily accessible (4).

Imamov and Pinsker (7) obtained the atomic positions by means of electron diffraction from thin films. The reflection intensities were determined visually and the  $R$  factor was 0.23.

Shiojiri *et al.* (8) prepared polycrystalline films through the solid–solid reaction of tellurium films with silver films at room temperature. The structure of the stuetzite phase was determined by means of HREM and image simulation. The crystal data which were used for image simulation by these authors are doubtful, as, e.g., the 6j Wyckoff position is occupied (not statistically) by only one silver atom.

Peters (4) synthesized a single crystal of  $\text{Ag}_{4.53}\text{Te}_3$  and determined its crystal structure by means of X-ray diffraction, resulting in an  $R$  factor of 0.073.

## EXPERIMENTAL

Thin films of  $\text{Ag}_{4.53}\text{Te}_3$  were prepared in a conventional high vacuum system equipped with a liquid nitrogen cooled trap and having a basic pressure of less than  $2 \times 10^{-5}$  Pa. Silver films 10–30 nm in thickness (measured with an oscillating quartz crystal microbalance) were deposited onto NaCl crystals (001)-cleaved in air and rinsed with bidistilled water to improve epitaxy (14). Silver (99.99%, Balzers AG) was deposited at a substrate temperature of 100°C (measured with a constantan-Ni thermocouple)

<sup>1</sup> To whom correspondence should be addressed.

TABLE 1  
Literature Data for  $\text{Ag}_{5-x}\text{Te}_3$

Composition	Formula units per unit cell	Lattice constants (nm)	Space group	Ref.
$\text{Ag}_{4.53}\text{Te}_3$	14	$a = 1.346$ $c = 1.690$	$\bar{P}62m$	(4)
		$a = 1.338$ $c = 0.849$		(5)
$\text{Ag}_7\text{Te}_4$	5	$a = 1.348$ $c = 0.849$	$P6/mmm$	(7)
$\text{Ag}_{32}\text{Te}_{27}$	1	$a = 1.340$ $c = 0.840$	$P6/mmm$	(8)
$\text{Ag}_{12}\text{Te}_7$	3	$a = 1.343$ $c = 0.845$		(9)
$\text{Ag}_5\text{Te}_3$	7	$a = 1.346$ $c = 0.846$	$C6/mmm$	(10)
$\text{Ag}_5\text{Te}_3$	7	$a = 1.346$ $c = 0.847$		(11)
$\text{Ag}_{5-x}\text{Te}_3$	7	$a = 1.349$ $c = 0.848$	$P6/mmm$	(12)
$\text{Ag}_5\text{Te}_3$	7	$a = 1.338$ $c = 0.845$	$C6/mmm$	(13)

from a tungsten boat at a rate of 1 nm/s. Tellurium (99.999%, Fluka) was then sublimated from a tungsten boat onto the silver layers at a substrate temperature of 25°C

TABLE 2  
Crystal Data of  $\text{Ag}_{4.53}\text{Te}_3$  (4) and  $\text{Ag}_5\text{Te}_3$  ( $\bar{P}62m$ ,  $a = 1.346$  nm,  $c = 1.690$  nm)

Atoms	Wyckoff positions	x	y	z	Occupation $\text{Ag}_{4.53}\text{Te}_3$	Occupation $\text{Ag}_5\text{Te}_3$
Te(1)	3g	0.6898	0.0000	0.5000	1.00	1.00
Te(2)	4h	0.3333	0.6666	0.1103	1.00	1.00
Te(3)	3f	0.3431	0.0000	0.0000	1.00	1.00
Te(4)	4h	0.3333	0.6666	0.3875	1.00	1.00
Te(5)	12l	0.1785	0.3004	0.2496	1.00	1.00
Te(6)	6i	0.4301	0.0000	0.2520	1.00	1.00
Te(7)	3g	0.3252	0.0000	0.5000	1.00	1.00
Te(8)	2e	0.0000	0.0000	0.4185	1.00	1.00
Te(9)	3f	0.6757	0.0000	0.0000	1.00	1.00
Te(10)	2e	0.0000	0.0000	0.1398	0.67	0.67
Te(11)	2e	0.0000	0.0000	0.0810	0.33	0.33
Ag(1)	6k	0.5651	0.4294	0.5000	0.80	0.92
Ag(2)	3f	0.8753	0.0000	0.0000	0.64	0.73
Ag(3)	12l	0.5400	0.3448	0.2476	1.00	1.00
Ag(4)	6i	0.1970	0.0000	0.1170	0.77	0.88
Ag(5)	6i	0.1947	0.0000	0.3701	0.98	0.98
Ag(6)	12l	0.2079	0.4220	0.4020	0.76	0.87
Ag(7)	6i	0.5756	0.0000	0.3624	0.74	0.85
Ag(8)	6j	0.5830	0.1470	0.0000	0.39	0.45
Ag(9)	12l	0.2163	0.4157	0.0963	0.67	0.77
Ag(10)	12l	0.1590	0.4510	0.1330	0.18	0.20
Ag(11)	12l	0.1510	0.4500	0.3660	0.18	0.20
Ag(12)	12l	0.5440	0.0460	0.1081	0.25	0.29
Ag(13)	6i	0.5610	0.0000	0.1310	0.50	0.57

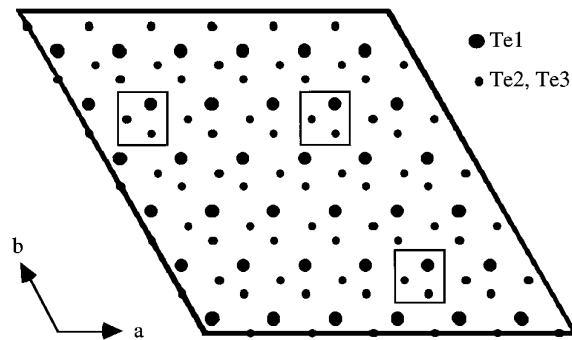


FIG. 1. Crystal structure of tellurium projected parallel to  $[001]$ ,  $6 \times 6 \times 6$  unit cells.

and at a rate of 1 nm/s. After wet stripping in bidistilled water, the samples were collected on holey carbon films on copper specimen grids and investigated in an electron microscope Hitachi HU-125S operating at 75 kV for selected area electron diffraction (SAED) and in a JEOL 200CX at 200 kV ( $C_s = 1.2$  mm) for HREM observations. Simulated images were calculated by the EMS (15) and MacTempas programs. Optical diffraction patterns were obtained with a laser diffractometer, built according to Refs. (16, 17).

#### CRYSTAL STRUCTURE DATA OF $\text{Ag}_{4.53}\text{Te}_3$

Crystal data given by Imamov and Pinsker (7) and by Peters (4) were used to simulate HREM images and those by Peters (4) to draw the crystal structure. Because the latter are not easily accessible, they are listed in Table 2.

Except for Ag(3), all silver atoms are statistically distributed.  $\text{Ag}_{4.53}\text{Te}_3$  represents a phase of structural cation disorder that is stable at room temperature.

Doubling of the unit cell can only be explained by the positions of the tellurium atoms Te(10) along  $[00z]$  because the distributions of the other tellurium atoms are identical in both of the subcells ( $c/2$ ).

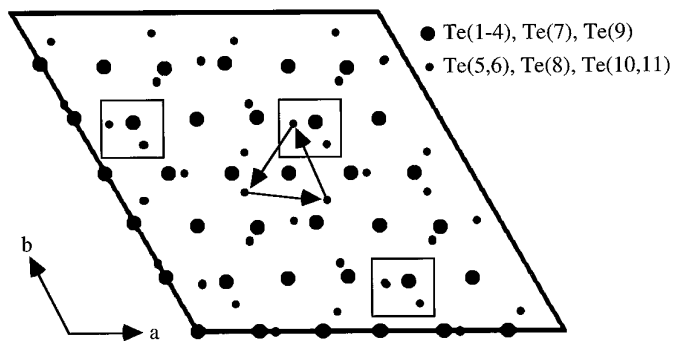


FIG. 2. Tellurium sublattice of  $\text{Ag}_{4.53}\text{Te}_3$  projected parallel to  $[001]$ ,  $2 \times 2 \times 2$  unit cells.

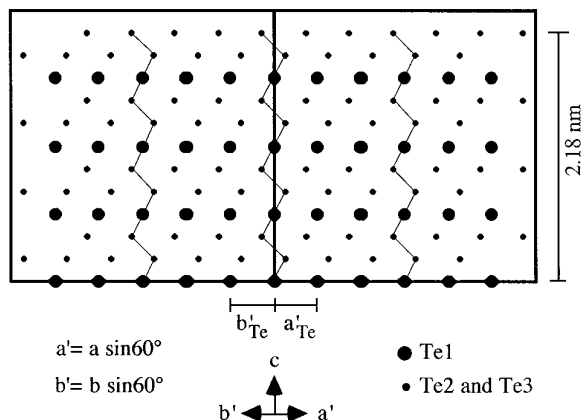


FIG. 3. Projection of the tellurium crystal structure parallel to  $[110]$ ,  $6 \times 6 \times 4$  unit cells, the tellurium atoms of the chains belong to the tellurium atoms in the framed areas of Fig. 1.

The lengths of the axes  $a$  and  $b$  of elemental tellurium ( $P3_121$ ,  $P3_221$ ) amount to 1.337 nm if multiplied by a factor of 3 (18). The lengths of the same axes are 1.346 nm for  $\text{Ag}_{4.53}\text{Te}_3$ . Comparing the lattice of tellurium (Fig. 1) with the Te partial lattice of  $\text{Ag}_{4.53}\text{Te}_3$  (Fig. 2) along the axes  $a$  and  $b$  shows that every third spiral chain of tellurium is retained in the Te sublattice of  $\text{Ag}_{4.53}\text{Te}_3$  (framed areas in Figs. 1 and 2).

If the spiral shaped chains of Te atoms in elemental tellurium are compared to those in  $\text{Ag}_{4.53}\text{Te}_3$ , the following is observed:

- every third chain of Te is found as well in the Te-sublattice of  $\text{Ag}_{4.53}\text{Te}_3$  in an identical position (Figs. 1 to 4).
- the chains of the stuetzite phase are elongated by 36% parallel  $[00z]$  in comparison to tellurium (Figs. 3 and 4).
- in contrast to tellurium, the spiral chains in  $\text{Ag}_{4.53}\text{Te}_3$  are rotated relative to each other by  $120^\circ$  (arrows in Fig. 2). This rotation is due to the fact that the threefold screw axis is absent in  $\text{Ag}_{4.53}\text{Te}_3$ .

### SAED CHARACTERIZATION

By reacting 30 nm thick silver films with 32 nm tellurium, single crystalline  $\text{Ag}_{5-x}\text{Te}_3$  films could be prepared at room temperature. The interplanar spacings for the (100) and (010) planes amount to 1.164 nm (Fig. 5). This is in good agreement with the values published by Peters (4) who gave 1.165 nm each for  $d_{100}$  and  $d_{010}$ . In the SAED pattern (Fig. 5), the superstructure reflections (as compared to the basic Te structure) can be easily recognized.

### HREM CHARACTERIZATION

Based on the structural model of  $\text{Ag}_{4.53}\text{Te}_3$  (4), HREM images for a stoichiometric  $\text{Ag}_5\text{Te}_3$  have been calculated.

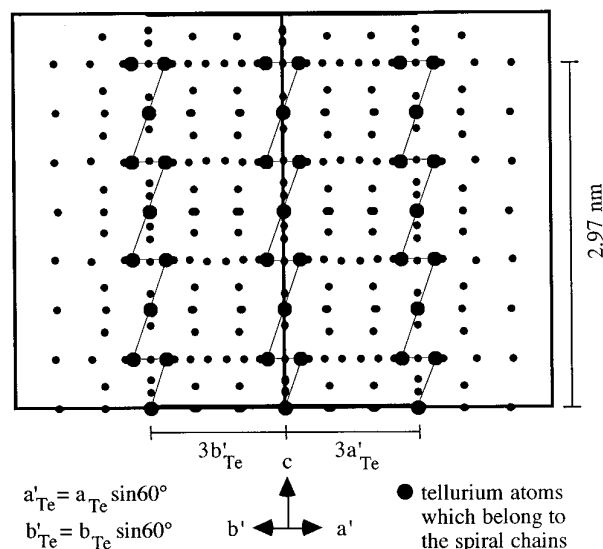


FIG. 4. Projection of the tellurium sublattice of  $\text{Ag}_{4.53}\text{Te}_3$  parallel to  $[110]$ ,  $2 \times 2 \times 2$  unit cells, the tellurium atoms of the chains belong to the tellurium atoms in the framed areas of Fig. 2.

It was assumed, that the tellurium sublattice of  $\text{Ag}_{4.53}\text{Te}_3$  is conserved in  $\text{Ag}_5\text{Te}_3$ . Except for Ag(3) and Ag(5), the occupation of the silver positions of  $\text{Ag}_{4.53}\text{Te}_3$  was increased to reach stoichiometric  $\text{Ag}_5\text{Te}_3$  (Table 2). The increase in silver occupation was distributed proportionally to all other silver positions. Cell dimensions calculated

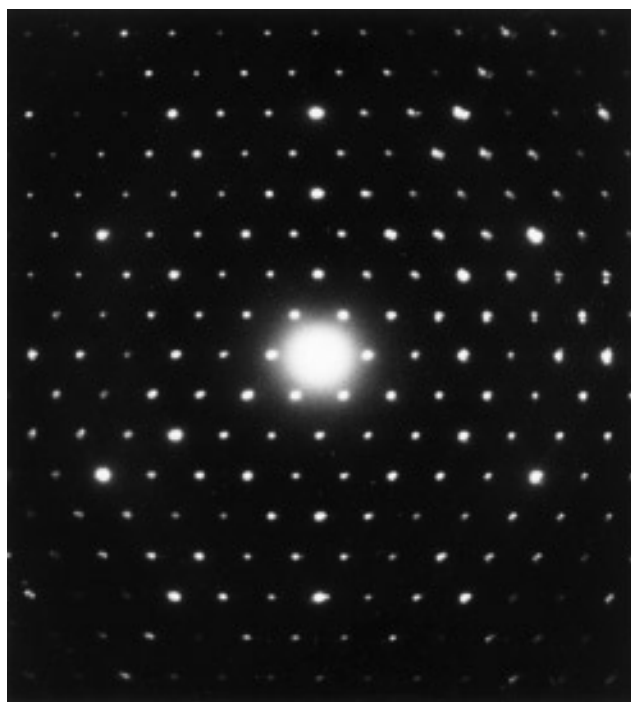


FIG. 5. SAED diffraction pattern of  $\text{Ag}_{5-x}\text{Te}_3$ ,  $[001]$  zone axis.

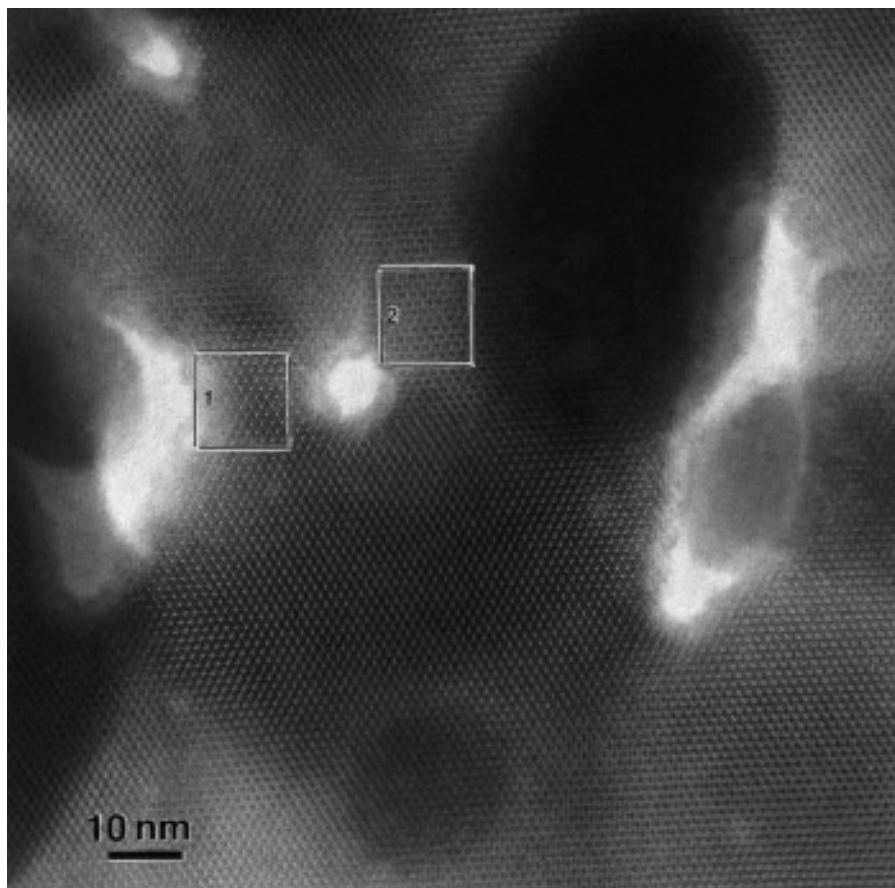


FIG. 6. HREM micrograph of  $\text{Ag}_{5-x}\text{Te}_3$ .

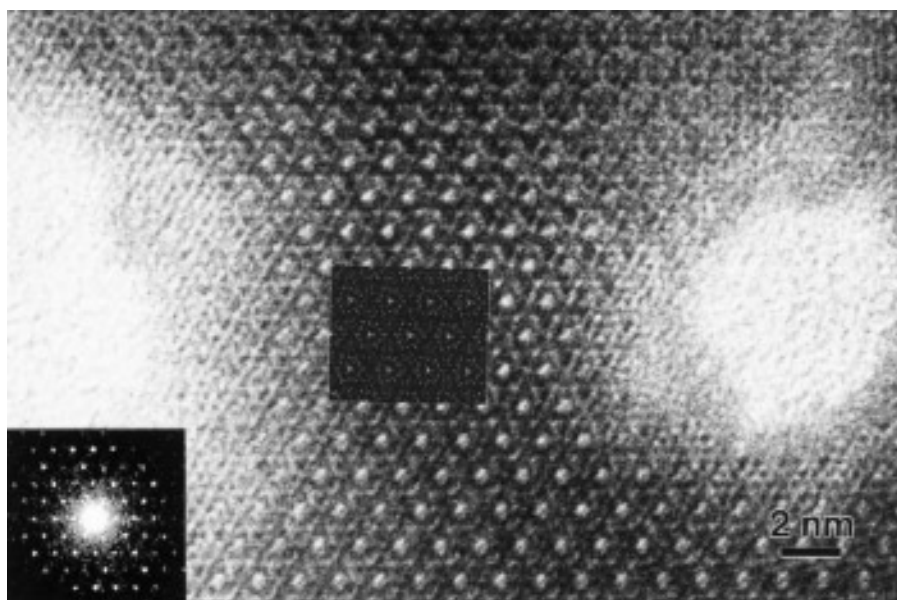


FIG. 7. Magnification of the framed area 1 in Fig. 6, [001] zone axis, defocus  $-85$  nm, thickness 11 nm. Insets: optical diffraction pattern and simulated image.

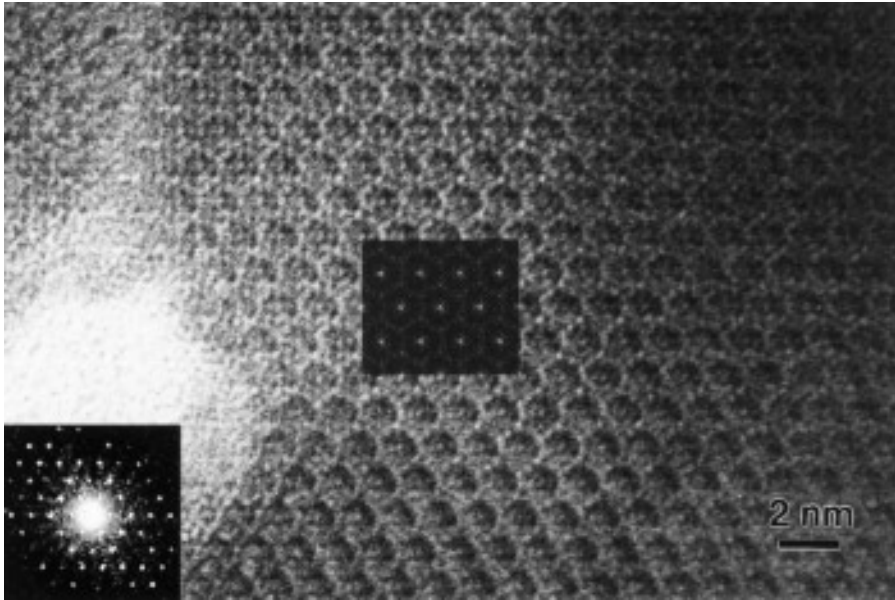


FIG. 8. Magnification of the framed area 2 in Fig. 6, [001] zone axis, defocus  $-25$  nm, thickness  $7.7$  nm. Insets: optical diffraction pattern and simulated image.

for Ag<sub>4.74</sub>Te<sub>3</sub> (11) and Ag<sub>4.95</sub>Te<sub>3</sub> (4) show no significant changes. The cell volume remains constant within the experimental limits of error. If the tellurium sublattice forms an almost close packed framework, random vacancies in the silver positions would not be expected to lead to measurable changes in the cell dimensions of Ag<sub>5</sub>Te<sub>3</sub> in comparison to Ag<sub>4.53</sub>Te<sub>3</sub>.

The reaction at room temperature of  $11$  nm tellurium with silver films  $10$  nm thick yielded polycrystalline hexagonal layers that were thin enough to be investigated by HREM and compared to simulated images.

Figure 6 shows an overview of such a film.

Micrographs of the areas enclosed by rectangles in Fig. 6 were taken at different defocus values (Figs. 7 to 10).

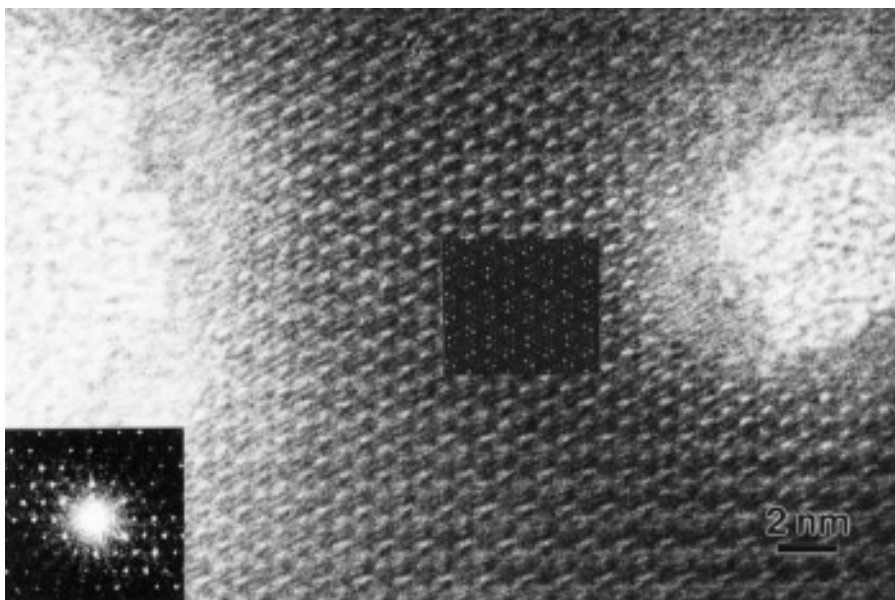


FIG. 9. Magnification on the framed area 1 in Fig. 6 [001] zone axis, defocus  $-160$  nm, thickness  $11$  nm. Insets: optical diffraction pattern and simulated image.

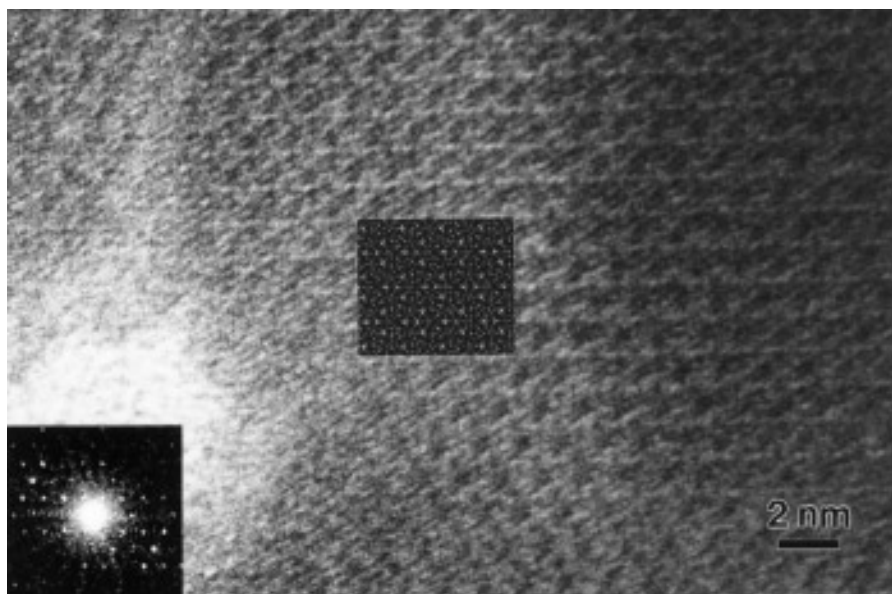


FIG. 10. Magnification of the framed area 2 in Fig. 6, [001] zone axis, defocus  $-100$  nm, thickness  $7.7$  nm. Insets: optical diffraction pattern and simulated image.

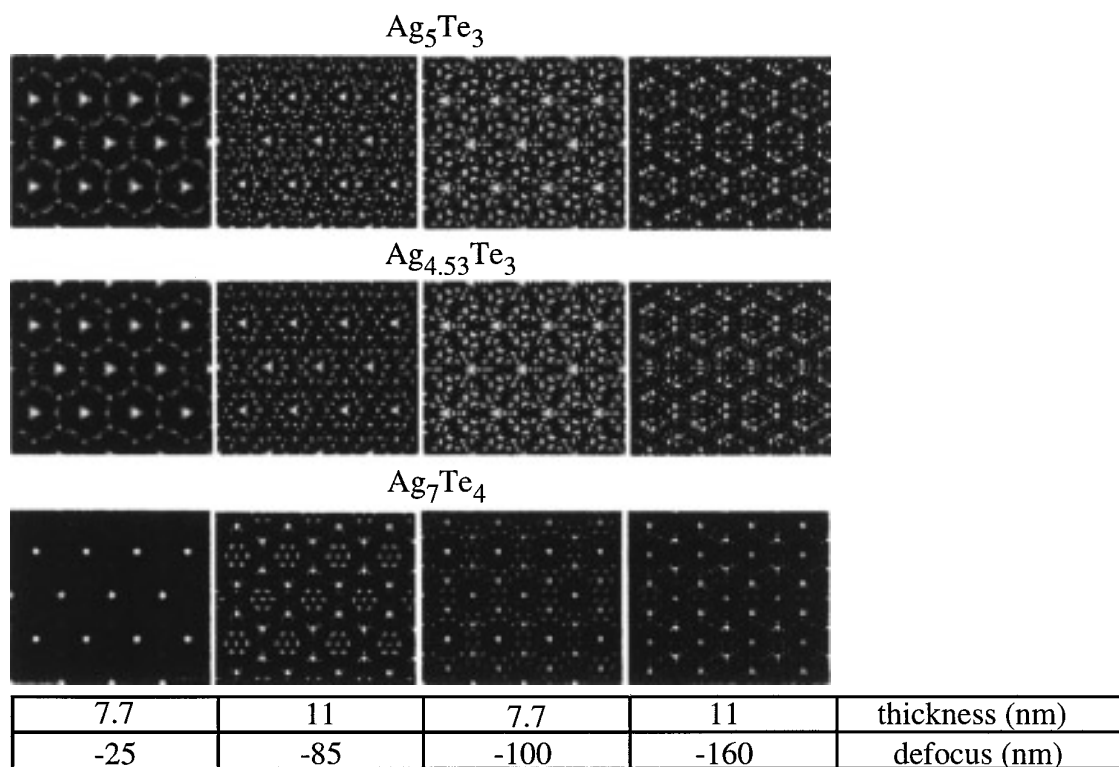


FIG. 11. Computer-simulated [001] images of  $\text{Ag}_5\text{Te}_3$ ,  $\text{Ag}_{4.53}\text{Te}_3$ , and  $\text{Ag}_7\text{Te}_4$  for different defocus values and crystal thicknesses.

Area 1 has a calculated thickness of 11 nm and area 2 of 7.7 nm. Based on the defocus values, it is found that areas 1 and 2 are shifted in the *z*-direction relative to each other. The different Gauss focus values of these two areas are caused by a slight buckling of the copper grids.

The calculated images for Ag<sub>4.53</sub>Te<sub>3</sub> and Ag<sub>5</sub>Te<sub>3</sub> are practically identical for defocus/thickness value pairs of -100 nm/7.7 nm and -160 nm/11 (Fig. 11).

At -25 nm/7.7 nm and -85 nm/11 nm, a small difference can be noticed, however. Based on this observation, we conclude that area 1 (Figs. 11 and 7) corresponds rather to Ag<sub>4.53</sub>Te<sub>3</sub> and area 2 (Figs. 11 and 8) to Ag<sub>5</sub>Te<sub>3</sub>.

For the structural model of Ag<sub>7</sub>Te<sub>4</sub> [7], HREM images have been calculated as well (Fig. 11, bottom line). They clearly indicate that this model does not correspond to the structure of the films studied here (Figs. 7 to 10).

Figure 7-10 show that the simulated images calculated from the model of Peters (4) give excellent agreement with experimental micrographs at different defocus values and film thicknesses, in contrast to the calculated images for Ag<sub>7</sub>Te<sub>4</sub> (7).

#### SUMMARY AND CONCLUSIONS

Single crystalline thin films of Ag<sub>5-x</sub>Te<sub>3</sub> have been prepared by the reaction of single crystalline silver films with tellurium vapor. A comparison of experimental high resolution electron micrographs with simulated images indicates that the structure of these films essentially corresponds to that given for Ag<sub>4.53</sub>Te<sub>3</sub> (4).

On the basis of the crystal structure of Ag<sub>4.53</sub>Te<sub>3</sub>, a model for a hypothetical, stoichiometric Ag<sub>5</sub>Te<sub>3</sub> was proposed. Thereby it has been assumed that the tellurium sublattice of Ag<sub>4.53</sub>Te<sub>3</sub> is conserved in Ag<sub>5</sub>Te<sub>3</sub>. The only partly occupied silver positions and the unoccupied positions were considered as solid solution. If the silver content of Ag<sub>4.53</sub>Te<sub>3</sub> is increased by 10.4% in this way, Ag<sub>5</sub>Te<sub>3</sub> is obtained.

It has been shown that under certain conditions (thickness, defocus) the image simulations allow an estimate

of the value *x* in Ag<sub>5-x</sub>Te<sub>3</sub>. Our films contain areas with different *x* values in the range 0.47 > *x* > 0. The structure determined by Peters (4) for bulk Ag<sub>4.53</sub>Te<sub>3</sub> proved to correctly represent that of our films as well.

Our results indicate that the structure of Ag<sub>5-x</sub>Te<sub>3</sub> (0 ≤ *x* < 0.5) can be described as an omission solid solution. This means that depending on the preparation conditions, *x* can adopt values from 0 to 0.5 without fundamental change of the structure over this entire range of stoichiometry.

#### REFERENCES

1. H. Haefke, A. Panov, and V. Dimov, *Thin Solid Films* **188**, 133 (1990).
2. J. R. Günter and P. Keusch, *Ultramicroscopy* **49**, 293 (1993); P. Keusch, Ph.D. Thesis. University of Zurich, 1992.
3. W. Kälin, Ph.D. Thesis. University of Zürich, 1995.
4. J. Peters, Ph.D. Thesis. Westfälische Wilhelms-Universität, Münster, 1982; J. Peters, O. Kourad, and B. Krebs, *Z. Anorg. Allg. Chem.*, in press.
5. C. Ching-Liang, R. M. Imamov, and Z. G. Pinsker, *Sov. Phys. Crystallogr.* **6**, 618 (1961).
6. M. Gobec and W. Sitte, *J. Alloys Compounds* **220**, 152 (1995).
7. R. M. Imamov and Z. G. Pinsker, *Sov. Phys. Crystallogr.* **11**, 182 (1966).
8. M. Shiojiri, T. Isshiki, Y. Hirota, and K. Okashita, *Bull. Inst. Chem. Res. Kyoto Univ.* **66**, 517 (1989).
9. V. Koern, *Naturwissenschaften* **27**, 23 (1939).
10. R. M. Thompson, M. A. Peacock, J. F. Rowland, and L. G. Berry, *Am. Mineral.* **36**, 458 (1951).
11. G. Donnay, F. C. Kracek, and W. R. Rowland, *Am. Mineral.* **41**, 722 (1956).
12. L. G. Berry and R. M. Thompson, *Geol. Soc. Am. Mem.* **85**, 1 (1962).
13. R. M. Honea, *Am. Mineral.* **49**, 325 (1964).
14. G. Safran, P. Keusch, J. R. Günter, and P. B. Barna, *Thin Solid Films* **215**, 147 (1992).
15. P. A. Stadelmann, *Ultramicroscopy* **21**, 131 (1987).
16. B. E. P. Beeston, R. W. Horne, and R. Markham, in "Electron Diffraction and Optical Diffraction Techniques" (A. M. Glauert, Ed.). North-Holland, Amsterdam, 1973.
17. J. C. H. Spence, in "Experimental High Resolution Electron Microscopy" (C. E. H. Bawn, H. Fröhlich, P. B. Hirsch, and N. F. Mott, Eds.). Clarendon, Oxford, 1981.
18. C. Adenis, V. Langer, and O. Lindqvist, *Acta Crystallogr. Sect. C* **45**, 941 (1989).